Acta Crystallographica Section B
Structural Science
ISSN 0108-7681

On the transferability of QTAIMC descriptors derived from X-ray diffraction data and DFT calculations: substituted hydropyrimidine derivatives

A. A. Rykounov,[a]* A. I. Stash,[b] V. V. Zhurov,[c] E. A. Zhurova,[c] A. A. Pinkerton[c] and V. G. Tsirelson[a]

[a]Mendeleev University of Chemical Technology, 9 Miusskaya Square, Moscow 125047, Russian Federation, [b]Karpov Institute of Physical Chemistry, 10 Vorontsovo Pole, Moscow 105064, Russian Federation, and [c]Department of Chemistry, University of Toledo, Toledo, OH 43606, USA

Correspondence e-mail: rykounov@muctr.ru

Received 9 June 2011
Accepted 15 August 2011

The combined study of electron-density features in three substituted hydropyrimidines of the Biginelli compound family has been fulfilled. Results of the low-temperature X-ray diffraction measurements and density functional theory (DFT) B3LYP/6-311++G** calculations of these compounds are described. The experimentally derived atomic and bonding characteristics determined within the quantum-topological theory of atoms in molecules and crystals (QTAIMC) were demonstrated to be fully transferable within chemically similar structures such as the Biginelli compounds. However, for certain covalent bonds they differ significantly from the theoretical results because of insufficient flexibility of the atom-centered multipole electron density model. It was concluded that currently analysis of the theoretical electron density provides a more reliable basis for the determination of the transferability of QTAIMC descriptors for molecular structures. Empirical corrections making the experimentally derived QTAIMC bond descriptors more transferable are proposed.

1. Introduction

This work describes the electron density (ED) features of the substituted hydropyrimidine derivatives belonging to the Biginelli (1893) class of compounds used as antihypertensive agents (Atwal *et al.*, 1991; Grover *et al.*, 1995), mitotic kinesin Eg5 inhibitors (Haggarty *et al.*, 2000) and α_{1a} adrenergic receptor-selective antagonists (Nagarathnam *et al.*, 1999; Barrow *et al.*, 2000). Previous studies of these compounds have focused mainly on exploration of their structure–activity relationships for the purpose of drug design (Rovnyak *et al.*, 1995; Shishkin *et al.*, 1997; Kappe *et al.*, 1997, 2000; Fabian *et al.*, 1998; Uray *et al.*, 2001; Gurskaya *et al.*, 2003*a*,*b*; Potemkin *et al.*, 2008). In this regard it is particularly important to establish how the ED characteristics of the Biginelli compounds are modified when they undergo conformational change. It is also necessary to study to what extent the ED features, determined for some specific conformation, can serve as transferable quantities suitable for the prediction of the chemical properties of other Biginelli compounds.

There are a few approaches which focus on *a priori* modeling of the electron density and related properties of molecules and crystals with a specified atomic structure, provided that the electron-density distributions of some fragments or of other conformers of the systems under study are known. The approaches differ in their goals and methods. The first one aims to reconstruct the ED with a multipole model by means of parameters obtained for individual pseudoatoms in specific valence states. These parameters are taken from data banks which are based either on averaging

over a number of high-resolution X-ray diffraction experiments (Pichon-Pesme *et al.*, 1995; Jelsch *et al.*, 1998; Housset *et al.*, 2000; Lecomte *et al.*, 2005; Zarychta *et al.*, 2007) or fitting the multipole model to structure factors obtained from a high-level non-empirical many-electron wavefuncton (Abramov *et al.*, 1999; Koritsanszky *et al.*, 2002; Volkov *et al.*, 2004, 2007; Coppens & Volkov, 2004; Dominiak *et al.*, 2007; Kalinowski *et al.*, 2007; Dittrich *et al.*, 2004; Hübschle *et al.*, 2007). The second approach focuses primarily on new drug discovery by means of quantitative structure–activity relationship (QSAR)/quantitative structure–property relationship (QSPR) methods. This family of fragment-based reconstruction techniques uses either the electron density itself (Walker & Mezey, 1994; Walker *et al.*, 1991; Zefirov & Palyulin, 2002) or ED-based molecular properties (Breneman & Rhem, 1997; Whitehead *et al.*, 2003; Breneman & Wiberg, 1990; Matta & Arabi, 2011). The third approach is based on the Quantum Theory of Atoms in Molecules and Crystals (QTAIMC; Bader, 1990, 2005). It provides meaningful physical and chemical information about such structural elements as atoms, chemical bonds and atomic groups, and makes possible the estimation of the properties of new compounds using available results obtained for the same class of molecule (Wiberg *et al.*, 1987; Chang & Bader, 1992; Matta & Bader, 2003; Popelier, 1999; O'Brien & Popelier, 1999, 2001). QTAIMC allows the description of the features of the ED distribution derived from both accurate X-ray diffraction measurements and non-empirical quantum chemical calculations in a uniform way, and therefore is commonly applied to characterize both intra- and intermolecular interactions in a wide variety of compounds, including bioactive compounds such as genetically encoded amino acids (Matta & Bader, 2000, 2002, 2003; Flaig *et al.*, 2002; de Carvalho *et al.*, 2007; Pakiari *et al.*, 2008), peptides (Lorenzo *et al.*, 2006; Vener *et al.*, 2007), DNA bases (Hübschle *et al.*, 2008; Gonzalez Moa *et al.*, 2008), alkaloids (Scheins *et al.*, 2005; Rincon *et al.*, 2009), natural estrogens (Zhurova, Matta *et al.*, 2006), large biomolecules such as NAD^+ and β-nicotinamide adenine dinucleotide (Guillot *et al.*, 2003), and vitamins (Milanesio *et al.*, 1997; Dittrich *et al.*, 2007).

Rykounov & Tsirelson (2009) have recently investigated the electron density and electronic energy properties of three functionally substituted hydropyrimidines (1), (2) and (3) (Fig. 1) applying QTAIMC to the density obtained from theoretical B3LYP/6-311++G** calculations. They quantitatively estimated the transferability of both local QTAIMC descriptors calculated at bond-critical points (the electron density, the Laplacian of the ED, kinetic, potential and electronic energy densities), and integrated ones (atomic volumes, charges and electronic energies). Tsirelson *et al.* (2006) also made an accurate joint low-temperature X-ray diffraction and non-empirical quantum chemical study of bonding in (3), and obtained extensive bond and atomic quantum-topological descriptors. A comparison of the QTAIMC results obtained for (3) from accurate X-ray diffraction measurements, three-dimensional periodic calculations (*CRYSTAL*98; Saunders *et al.*, 1998) and single-molecule DFT B3LYP/6-311G(d,p) calculations confirmed earlier findings (Chandler & Spackman, 1982; Parini *et al.*, 1985; Iversen *et al.*, 1997; de Vries *et al.*, 2000; Volkov *et al.*, 2000; Volkov & Coppens, 2001; Flaig *et al.*, 2002; Bytheway *et al.*, 2002; Tsirelson *et al.*, 2006) that the main differences between the experimentally and theoretically obtained properties are observed for the longitudinal ('along the bond path') ED curvature, λ_3. This may be attributed to a deficiency of the ED description with current multipole models. This deficiency is much less substantial for atomic energy characteristics integrated within basins delimited by zero-flux boundaries, because the Laplacian term in the kinetic energy expression is zero in this case (Tsirelson, 2002). As a result, the atomic energy descriptors derived from experiment and quantum chemical calculations are generally in much better agreement than those at the bond-critical points (BCPs). Thus, it appears that the atomic QTAIMC descriptors are currently preferable for studying transferability in similar compounds.

In this article we report the results of the combined experimental and theoretical investigation of QTAIMC characteristics for (1) and (2). A new multipole model refinement using experimental data obtained for crystal (3) was also undertaken. In addition, we report the influence of the local environment through a gradual increase of the size of the system considered in the series single molecule–dimer–tetramer–crystal, on the BCP properties, and atomic volumes and charges for compounds of the same chemical class. It will be shown by comparison of experimental and theoretical data that *the bond* characteristics are strongly influenced by the multipole model. This is particularly noticeable in the most polar bonds. The descriptors of the constituent *atoms* of the hydropyrimidine heterocyclic ring, such as volumes and charges, are fully transferable, whereas the volumes of the terminal atoms are affected by the influence of the local environment and vary considerably. Ways of avoiding these problems are also discussed.

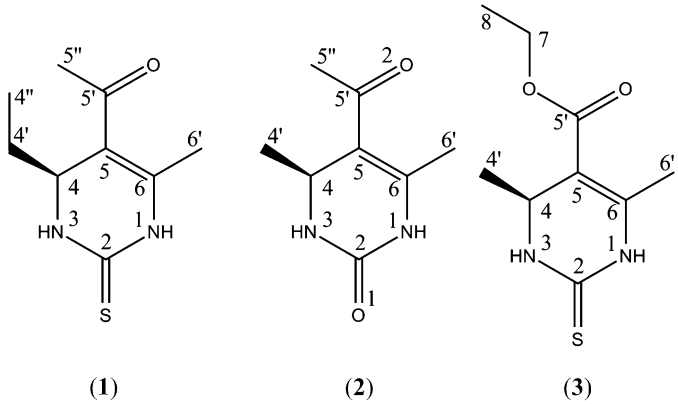

Figure 1
Molecular structures of 5-acetyl-4-ethyl-6-methyl-1,2,3,4-tetrahydropyrimidine-2-thione (1), 5-acetyl-4,6-dimethyl-1,2,3,4-tetrahydropyrimidine-2-one (2) and ethyl 4,6-dimethyl-2-thioxo-1,2,3,4-tetrahydropyrimidine-5-carboxylate (3).

Table 1
Experimental details.

Refinement was with 0 restraints.

	(1)	(2)
Crystal data		
Chemical formula	$C_9H_{14}N_2OS$	$C_8H_{12}N_2O_2$
M_r	198.28	168.20
Crystal system, space group	Triclinic, *P*1	Monoclinic, *C*2/*c*
Temperature (K)	110	110
a, *b*, *c* (Å)	7.2533 (2), 7.8212 (2), 9.1837 (3)	14.2785 (1), 6.9187 (1), 17.1827 (2)
α, β, γ (°)	97.187 (1), 100.674 (1), 94.106 (1)	90, 103.642 (1), 90
V (Å^3)	505.54 (2)	1649.56 (1)
Z	2	8
Radiation type	Mo $K\alpha$	Mo $K\alpha$
μ (mm^{-1})	0.28	0.10
Crystal size (mm)	0.40 × 0.22 × 0.14	0.42 × 0.34 × 0.22
Data collection		
Diffractometer	Bruker diffractometer with a SMART 6000 CCD detector	Bruker diffractometer with a SMART 6000 CCD detector
Absorption correction	Multi-scan (Blessing, 1995)	None
T_{min}, T_{max}	0.909, 1.106	–
No. of measured, independent and observed [$I > 2\sigma(I)$] reflections	57 560, 12 868, 10 974	46 839, 8718, 7330
R_{int}	0.042	0.048
Completeness (%)	97.2	94.2
Spherical refinement		
Reflections used ($I > 2\sigma$)	10 974	7330
Refinement based on	F^2	F^2
$R[F^2 > 2\sigma(F^2)]$, $wR(F^2)$, S	0.030, 0.086, 1.082	0.035, 0.105, 1.067
Multipole refinement		
No. of reflections ($I > 3\sigma$)	10 418	6921
No. of parameters	275	228
Refinement based on	F^2	F
Weighting scheme	$w = 1/[\sigma^2(F^2) + 0.03(F^2) + 2.5P]$, where $P = (F_o^2 + 2F_c^2)/3$	$w = 1/[\sigma^2(F^2) + 0.00015(F^2)]$
$R[F > 3\sigma(F)]$, $wR(F)$, S	0.0188, 0.0303, 1.343	0.0189, 0.0224, 1.071
$\Delta\rho_{min}$, $\Delta\rho_{max}$ (e Å^{-3})	−0.134, 0.137	−0.138, 0.148

Computer programs used: *SMART*, *SAINT* (Siemens, 1996), *SORTAV* (Blessing, 1987, 1989, 1995), *SHELXS*97, *SHELXL*97 (Sheldrick, 2008), *MOLDOS*97/*MOLLY* (Protas, 1997).

2. Experimental

2.1. Data collection and reduction

Compounds (1) and (2) were synthesized by Dr Shutalev as described by Shutalev & Kuksa (1997) and Shutalev *et al.* (1998). Single crystals used in the accurate X-ray structure analysis were grown by slow evaporation of a saturated solution of these compounds in ethanol at room temperature. Prismatic colorless samples were mounted on the top of a 0.1 mm capillary and slowly cooled to 110 K with an Oxford Cryostream system. The X-ray diffraction experiment was performed using a Bruker Platform diffractometer with a SMART 6000 area CCD detector. Data were collected with the ω scan method (0.3° ω step) and detector distances of 5.24 cm for crystal (1) and 6.10 cm for (2). Two detector positions $2\theta = -15$ and $-75°$ and several different φ settings were used.

Data integration and unit-cell determination were performed with the program *SAINT* (Siemens, 1996). The integration box was chosen empirically. The profile fitting procedure based on strong reflections provided good internal consistency, $R_{int} = 0.042$ for (1) and 0.048 for (2). The data were scaled and merged with the program *SORTAV* (Blessing, 1987, 1989). A multi-scan absorption correction was applied for (1) (Blessing, 1995). Other experimental details for (1) and (2) are given in Table 1.

2.2. Refinement

First, the structures of (1) and (2) (Figs. 2 and 3) were refined with the *SHELXTL* program suite (Sheldrick, 2008) using the spherical-atom model starting from the room-temperature structural parameters from Zavodnik *et al.* (2005*a*,*b*). The atomic relativistic scattering factors and anomalous scattering corrections were taken from *International Tables for Crystallography* (1995). The atomic displacements for all atoms except H atoms were treated anisotropically. No extinction was found for either crystal. The atom-centered multipole model (Hansen & Coppens, 1978) was used in a subsequent refinement. The Macchi & Coppens (2001) atomic relativistic wavefunctions calculated at the multiconfiguration Dirac–Fock level were used to describe both core and valence densities for each atom. The valence-density multipoles were described up to the octupole level for C, N, O and S atoms, while only dipoles were refined for H atoms. The inclusion of higher multipoles did not change the electron density meaningfully, and they were not considered further.

The multipole refinements based on F^2 for (1) and $|F|$ for (2) with least-squares weighting schemes specified in Table 1 were performed using the program *MOLDOS*2004 (Stash, 2003) modified from *MOLLY* (Hansen & Coppens, 1978) and *MOLDOS*97 (Protas, 1997). The C—H and N—H distances were elongated up to their standard recommended values (*International Tables for Crystallography*, 1995) to provide a more accurate description. The atomic positional and anisotropic displacement parameters of the non-H atoms were refined using data with $\sin\theta/\lambda > 0.65$ Å^{-1}. The isotropic displacement parameters of the H atoms were refined in the low-angle region ($\sin\theta/\lambda < 0.65$ Å^{-1}). The multipole refine-

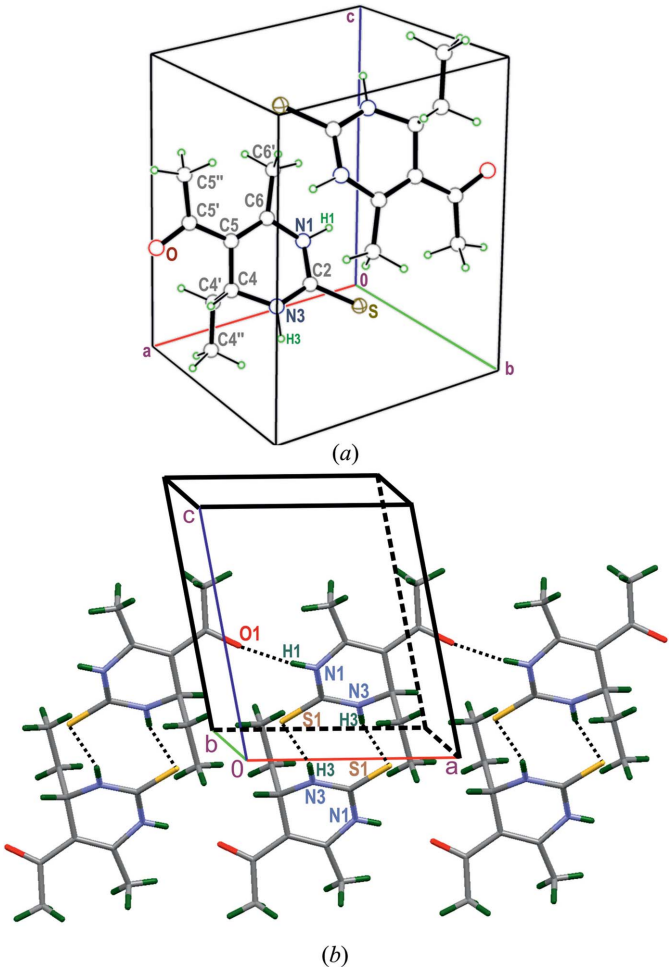

Figure 2
View of (*a*) the crystal packing (*ORTEP*III; Burnett & Johnson, 1996) and (*b*) intermolecular interactions in (1).

ments were carried out using the complete data sets; details are given in Table 1. Multipole parameters for (3) were re-refined using the same refinement strategy as for (2) [$R(F) = 0.0192$, $wR(F) = 0.0217$ and $S = 1.17$].

The quasi-static electron density reconstructed from the multipole parameters appeared to be positive everywhere for all three compounds. The residual distributions in (1) and (2) did not show any meaningful features except for random positive areas ~ 0.1 e Å^{-3} observed near the O atoms attached to C5′ for both compounds, and near the double C5═C6 bond in (2). The residual distribution for (3) had no significant features either. The average residual density values were 0.040 e Å^{-3} for (1), 0.038 e Å^{-3} for (2) and 0.05 e Å^{-3} for (3). The ED errors in the middle of the bonds computed from the s.u.'s of the multipole model parameters (Tsirelson & Ozerov, 1996) did not exceed 0.05 e Å^{-3} and were within the residual noise for all bond types. The residual electron-density maps for (1) and (2) have been deposited (Fig. 1S)[1] as well as the results of the Hirshfeld rigid-bond test (Hirshfeld, 1976), which demonstrated that the displacement parameters for non-H atoms were unbiased (Table S1). The reconstruction of the electron density and the Laplacian of the ED from the multipole model, and extensive topological analysis of the reconstructed density have been performed with the program *WinXPRO*; Stash & Tsirelson, 2002, 2005)

2.3. Theoretical calculations

All quantum-chemical calculations for monomers, dimers and tetramers (Fig. 2S–4S) were performed with the *GAUSSIAN*03 program package (Frisch *et al.*, 2003). Geometry optimizations and many-electron wavefunction determinations were performed at the B3LYP/6-311++G** level of theory. The choice of basis set was based on its successful application to reveal the intra- and intermolecular features of the electron density, the Laplacian of the electron density and the electronic energy density for medium-sized organic molecules (see, for example, Matta & Bader, 2002; Hibbs, Hanrahan *et al.*, 2003; Hibbs, Austin-Woods *et al.*, 2003; Castillo *et al.*, 2005; Matta *et al.*, 2006; Matta, 2010; Zhurova, Matta *et al.*, 2006; Zhurova, Stash *et al.*, 2006; Rykounov & Tsirelson, 2009). The geometrical parameters from the X-ray diffraction experiments were used as starting values for the calculations. The absence of imaginary frequencies for all the structures was confirmed by harmonic vibration frequency analysis. Thus, all obtained molecular structures correspond to

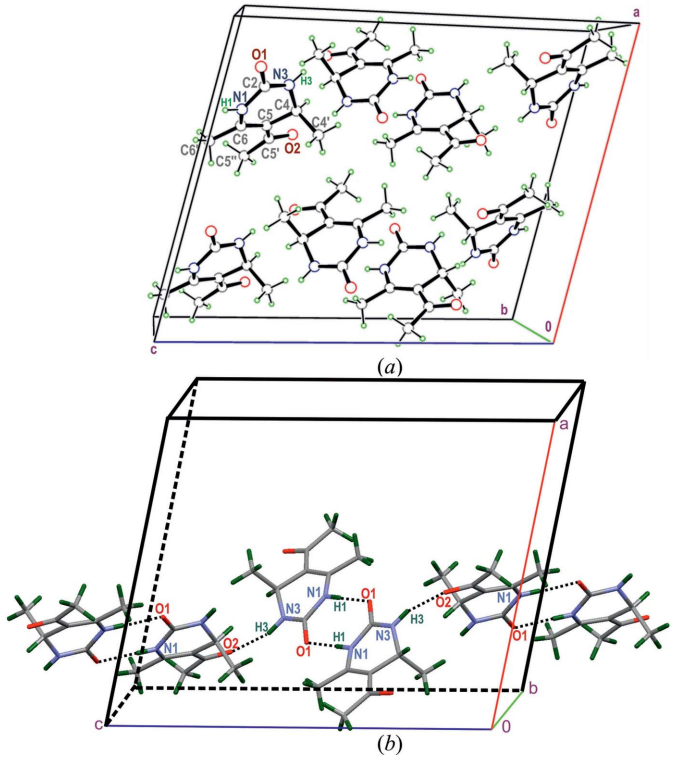

Figure 3
View of (*a*) the crystal packing (*ORTEP*III; Burnett & Johnson, 1996) and (*b*) intermolecular interactions in (2).

[1] Supplementary data for this paper are available from the IUCr electronic archives (Reference: EB5011). Services for accessing these data are described at the back of the journal.

the minima on the potential energy surfaces. The QTAIMC parameters for atoms and bonds in monomers, dimers and tetramers were determined using the *AIMAll* program package (Keith, 2009). The electron-density distribution in the crystals was computed with the *CRYSTAL*98 package at the experimental geometry and the topological properties were calculated using the program *TOPOND* (Gatti, 1999). In addition, the multipole model has been fitted to the structure factors obtained from the *CRYSTAL*98 (DFT, B3LYP/6-311G**) calculations, and the theoretical model-density features were obtained using the *WinXPRO* package to provide a comparison of the experimental and theoretical results derived using the same refinement procedure.

3. Results and discussion

3.1. Molecular and crystal structure

All three molecules (Fig. 1) consist of a six-membered non-saturated heterocyclic ring N1—C2(O,S)—N3—C4—C5═C6 with substituents in positions 4, 5 and 6, which differentiate the three structures. The ring exhibits a distorted boat conformation both in the crystal and the monomer, the N1 and C4 atoms deviating from the C2—N3—C5—C6 plane by up to 11 and 25°. The substituent in position 4 is an ethyl group in (1) and a methyl group in (2) and (3). There is an acetyl group in position 5 of the heterocyclic ring in (1) and (2), and a carboxyethyl group in (3). All three molecules have a methyl group in position 6. The C5′═O part of the carbonyl fragments, and the double C5═C6 bonds have an s-*trans* arrangement about the single C5—C5′ bonds.

Both N—H fragments of the heterocyclic ring in molecules (1) and (3) form intermolecular hydrogen bonds with the O atom of the carbonyl group (N1—H1···O) and the S atom of the thioxocarbonyl group (N3—H3···S) of another molecule (Fig. 2). The latter represents a pair of bonds which link the molecules into dimers which are then linked into chains by the former. The pattern in (2) is rather similar: two strong N3—H3···O interactions link molecules into dimers bonded with neighboring molecules by multiple interactions *via* the side chains.

Bond lengths for (1), (2) and (3) are in reasonable mutual concordance in both the crystal and gas-phase (Tables S2–S4). Typically, the deviations of bond lengths between non-H atoms do not exceed 0.015 Å.

3.2. Transferability of the bond-critical point characteristics

The electron density and the Laplacian of the ED at the bond-critical points (BCP), and their corresponding bond lengths are presented in Figs. 4–6 and Tables S2–S7 for intra- and intermolecular interactions in (1)–(3). The comparison of the BCP characteristics of covalent bonds for the molecules in the gas phase and the crystal shows that a difference in the bond lengths is not always accompanied by noticeable changes in the BCP parameters in (1), (2) and (3). This is in line with recent observations for transition-metal systems (Ponec & Gatti, 2009). At the same time, the difference in ED values between single-molecule and experimental results reaches 0.04 a.u. for the most polar bonds formed by N or O atoms. For other bond types, the experimental ED values at the BCPs are reasonably close to those from the single-molecule quantum-chemical calculations, deviations generally being less than 0.01 a.u.

The agreement of the Laplacian values at the BCPs from a single-molecule theoretical calculation and the experiment is significantly worse, as expected. This is mainly due to the above-mentioned deficiency of the current multipole models (Chandler & Spackman, 1982; Parini *et al.*, 1985; Iversen *et al.*, 1997; de Vries *et al.*, 2000; Volkov *et al.*, 2000; Volkov & Coppens, 2001; Bytheway *et al.*, 2002; Tsirelson *et al.*, 2006). The largest Laplacian differences have been observed for the polar double C═O bonds in both the acetyl and carboxyethyl 5-substituents, and for the carbonyl group in position 2 of the heterocyclic ring; the maximum difference of 1.36 a.u. is observed in (3). Significant Laplacian deviations of up to 0.51 a.u. have also been observed for the N—H bonds. The values of $\nabla^2\rho(r)$ are underestimated in the first case and overestimated in the second.

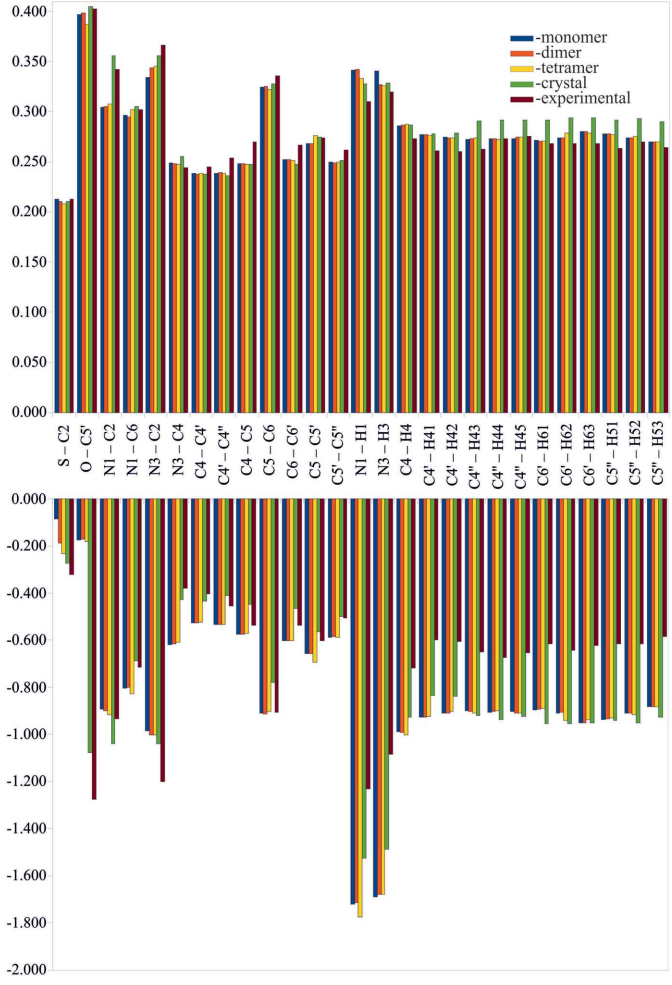

Figure 4
The electron density (a.u., up) and the Laplacian of the electron density (a.u., down) at the intramolecular BCPs of (1).

It has previously been reported (Dittrich *et al.*, 2003; Hübschle *et al.*, 2008; Destro *et al.*, 2008; Fournier *et al.*, 2009) that, for different compounds, the experimental Laplacian values at the bond-critical points are usually approximately 1 a.u. higher for a C═O bond and 0.5 a.u. lower for an N—H bond compared with the values derived from wavefunctions. As it is a general observation, the experimental multipole-model values should be corrected if they are to be used as transferable QTAIMC descriptors. Such corrections could be estimated from the observed differences between BCP characteristics obtained from the theoretical electron density and those computed from the multipole model fitted to experimental or theoretical structure factors. In the present case of substituted hydropyrimidine derivatives, the empirically corrected experimental Laplacian values for the above-mentioned bond types proved to be in much better agreement with the results from direct theoretical calculations.

Let us now consider to what extent the QTAIMC bond descriptors are transferable from the molecule and/or molecular cluster calculations to a crystal. We have compared the bond lengths and QTAIMC parameters of the atoms and covalent bonds from the B3LYP/6-311++G** calculations of the monomer, dimer and tetramer of (1), (2) and (3) with those for a crystal (Tables S2–S4). The bond lengths for covalent bonds involving the C2 atom, C2—N1, C2—N3 and C2═O(S), significantly change in the series monomer–dimer–tetramer–crystal. A significant elongation of the bonds in the dimers, tetramers and crystal compared with the monomers was observed. The N—H bond lengths in the dimers and tetramers are significantly increased with respect to both the crystal and the monomer.

For (1) the average deviation of the electron density at BCPs from experimental values is 0.012 a.u. in the monomers and 0.011 a.u. in the dimers. The largest ED difference between dimers and tetramers is 0.003 a.u. for the N1—C2 bond. For (2) the corresponding differences are 0.015 a.u. for the monomer and 0.014 for the dimer and tetramer. At the same time the maximum ED difference slightly increases from 0.047 to 0.048 and 0.057 a.u. with increasing cluster size. In (3) the average ED deviation is more significant for the dimer (0.011 a.u.) than for the monomer (0.002 a.u.); no further increase in the tetramer was found.

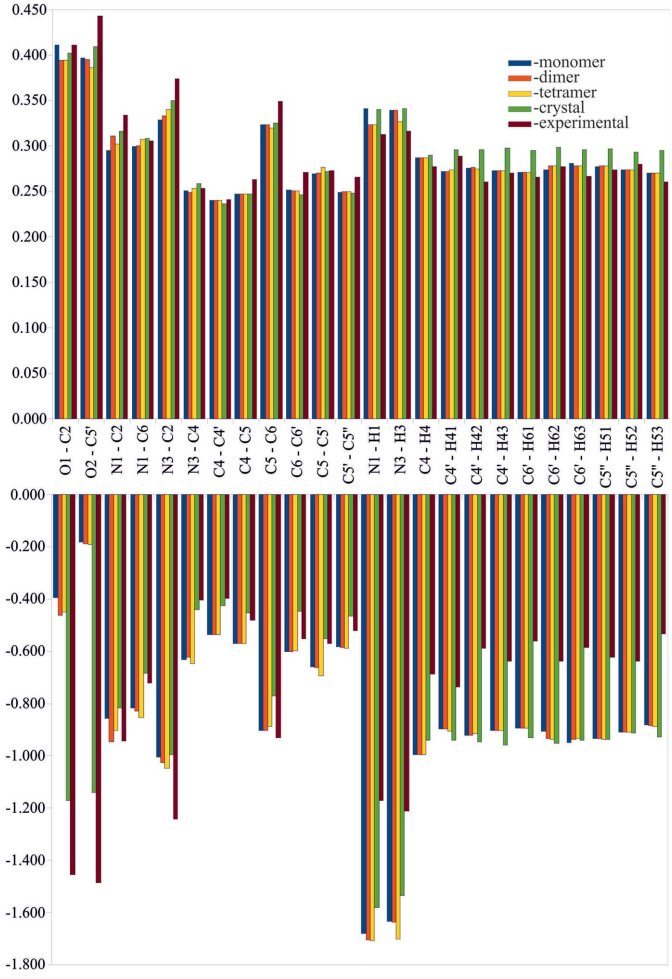

Figure 5
The electron density (a.u., up) and the Laplacian of the electron density (a.u., down) at the intramolecular BCPs of (2).

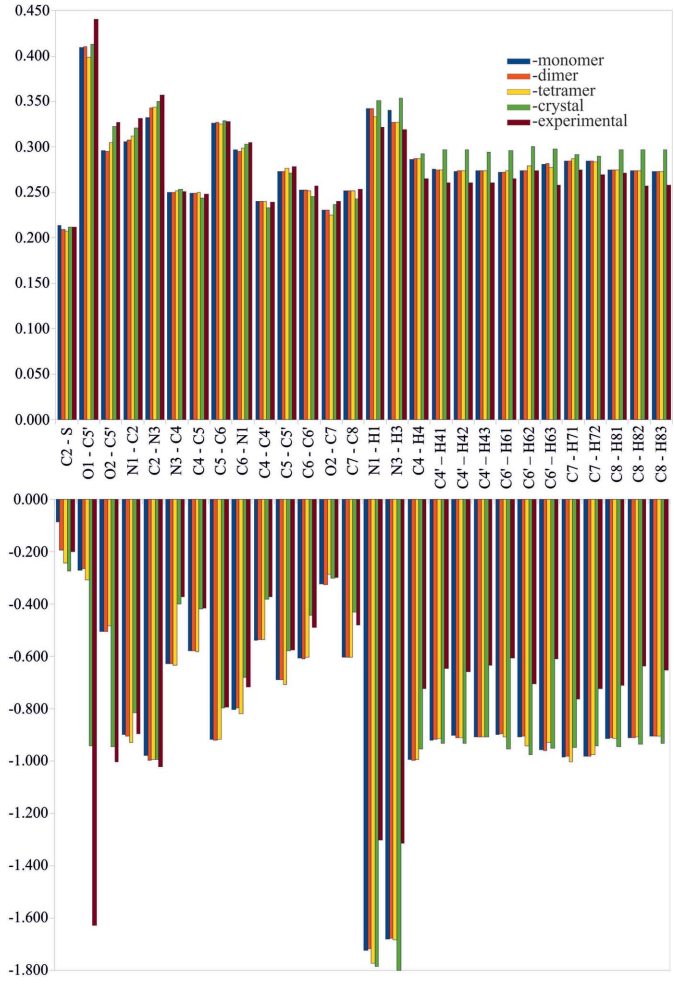

Figure 6
The electron density (a.u., up) and the Laplacian of the electron density (a.u., down) at the intramolecular BCPs of (3).

The values of $\nabla^2\rho(r)$ at the BCPs of C=O and N—H bonds change on going from a monomer to the molecular dimer and tetramer, all being quite different from the experimental values (Fig. 4–6). The intermolecular hydrogen bonds change the bond parameters in the heterocyclic ring in a rather unpredictable way. The consideration of a molecular dimer or tetramer just slightly improves the general agreement between theoretical and experimental results for these bonds.

Thus, neither monomer nor molecular cluster calculations provide the BCP descriptors which can be considered as transferable to a crystal (at least for substituted hydropyrimidines).

The distributions of the Laplacian of the electron density in the crystals of (1), (2) and (3) obtained from the multipole models fitted to both experimental and theoretical structure factors are shown in Fig. 7. The C2—C5—C6 plane reflects the main characteristic features of the Laplacian distribution. The conformations of the partially unsaturated heterocyclic rings in (1), (2) and (3) are non-planar, and the torsion angle C6—C5—C5′—O1 is not equal to 0 or 180°. Therefore, the O atom of the acetyl or carboxyethyl group deviates from the plane, and its Laplacian features look slightly different in the plane as drawn. In addition, the orientations of some bonds with respect to the planes shown in Fig. 7(*a*) result in noticeable ruptures in the negative Laplacian (see, for example, the substituent in position 5 of the heterocyclic ring in Figs. 7*b* and *c*). Taking into account these points, we can conclude that the

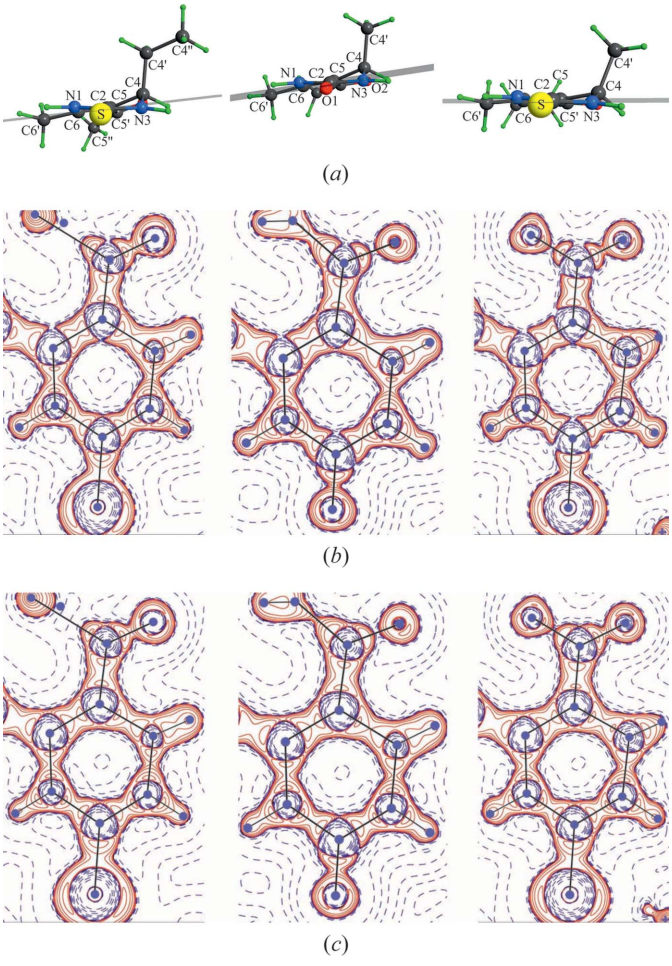

Figure 7
The Laplacian of the electron density in crystals (1), (2) and (3) obtained from the experimental and theoretical structure factors using the multipole model: (*a*) the planes through the C2—C5—C6 atoms in which the Laplacian is depicted; (*b*) experimental Laplacian map; (*c*) theoretical Laplacian map. Red solid lines denote the areas of electron-density concentration [$\nabla^2\rho(r) < 0$] and blue dashed lines correspond to electron density depletion. Contour intervals are $\pm 2, 4, 8 \times 10^n$ e Å^{-5} ($n = -3$ to 2).

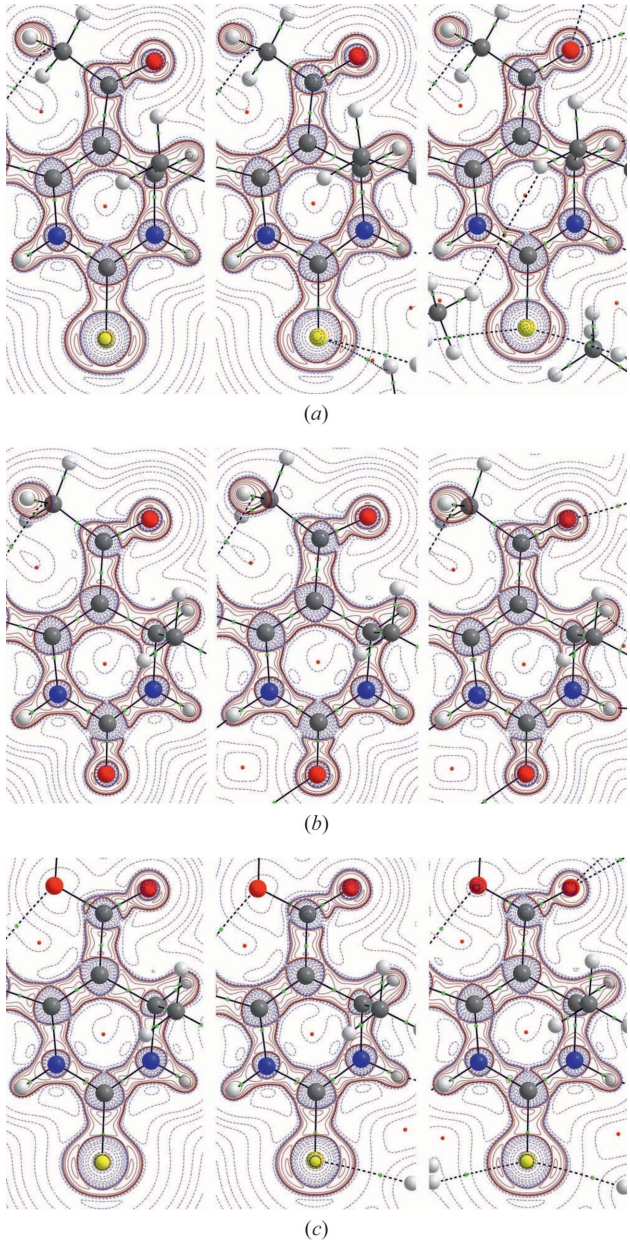

Figure 8
The Laplacian of the electron density in the C2—C5—C6 plane for molecules (*a*) (1), (*b*) (2) and (*c*) (3) obtained from theoretical calculations for the monomer, dimer and tetramer (from left to right). Solid red lines denote the areas of density concentration [$\nabla^2\rho(r) < 0$] and dashed blue lines correspond to density depletion. Contour lines are $\pm 2, 4, 8 \times 10^n$ e Å^{-5} ($n = -3$ to 2).

general pattern of the features of the Laplacian is essentially the same for the different compounds from the experiments and theoretical calculations.

The theoretical Laplacian maps for monomers, dimers and tetramers of (1), (2) and (3) are shown in Fig. 8. Again, the maps are very similar both for different clusters and different compounds. The negative Laplacian areas corresponding to the electron density concentration and to local domination of the potential energy are located along the covalent bonds and at the sites of the electron lone pairs of O and S atoms, as expected. The pattern of the Laplacian distribution inside the heterocyclic ring is remarkably similar for all nine structures. The electron density is locally depleted at the center of the ring as it is in benzene (Bürgi *et al.*, 2002).

The range of the Laplacian at the BCPs of the C5═C6 bonds is −(0.90–0.92) a.u. for both differently sized molecular clusters and different compounds (Tables S2–S4). Good agreement of the Laplacian is also observed for the N1—C2 and N3—C2 bonds as well as for the N—H bonds involved in the intermolecular interactions. Even for the carbonyl O and S atoms which additionally participate in weak interactions, the Laplacian distribution looks very similar, despite the slight deviation of these atoms from the plane. We thus conclude that non-covalent interactions such as hydrogen bonds or van der Waals interactions do not significantly change the picture of the *ab initio* theoretical Laplacian distribution in large clusters of (1), (2) and (3) in comparison to the monomer.

Figs. 7 and 8 show that the Laplacian of the electron density in Biginelli compounds is in semi-quantitative agreement between the same and different molecules within the framework of a chosen method – the experimentally fitted multipole model or quantum chemical calculations. The numerical BCP characteristics (Tables S2–S4) confirm that the quantum-topological descriptors of the heterocyclic ring bonds (the common moiety in all three compounds) are fully transferable when derived within the same approach. These conclusions are in line with the results obtained from earlier theoretical calculations on conformers of substituted hydropyrimidines (Rykounov & Tsirelson, 2009). To some extent the transferability of the quantum-topological descriptors will be preserved for other substituents in positions 4, 5 and 6 of the heterocyclic ring in Biginelli compounds. Local perturbations of the ED and related characteristics can be expected if the structure of a new substituent significantly differs from those in the compounds (1), (2) and (3).

Let us now consider the closed-shell inter- and intramolecular interactions and analyze how the quantum-topological properties of their BCPs differ between theory and experiment, and between different molecules. Three types of 'weak' interactions occurring in molecules, clusters and crystals of (1), (2) and (3) could be distinguished. The first is a closed-shell intramolecular interaction between the atoms of substituents in positions 5 and 6 of the heterocyclic ring. The difference in the theoretical electron density at the BCPs for the monomer, dimer, tetramer and with periodic boundary conditions (crystal) with respect to the experiment is ≤ 0.003 a.u. for this kind of interaction in all three compounds (Tables S5–S7). Surprisingly, the deviation of the Laplacian value is also quite small for this bond type: the values of $\nabla^2\rho(r)$ are the same for (1) and (2) and vary only by 0.01 a.u. in (3). We should mention here that for both closed-shell intramolecular interactions and intermolecular hydrogen bonds, the significant variations in the geometrical parameters are not accompanied by large changes in the ED. For example, the distance between C5″ and H63 in (2) differs by 0.46 Å between experiment and theory, while the electron density at the BCP on the C5″···H63 interaction line deviates only by 0.001 a.u. and the Laplacian value does not change at all.

The second type of non-covalent interaction is the intermolecular hydrogen bond between the H atom of an N—H residue and the O atom or its sulfur substitution in the carbonyl group in position 2 of the heterocyclic ring. The largest ED deviation from the experimental value (0.009 a.u.) is observed for the multipole model derived from theoretical structure factors in (1) and (2). For the molecular dimers and tetramers, the theoretical electron density differs from the

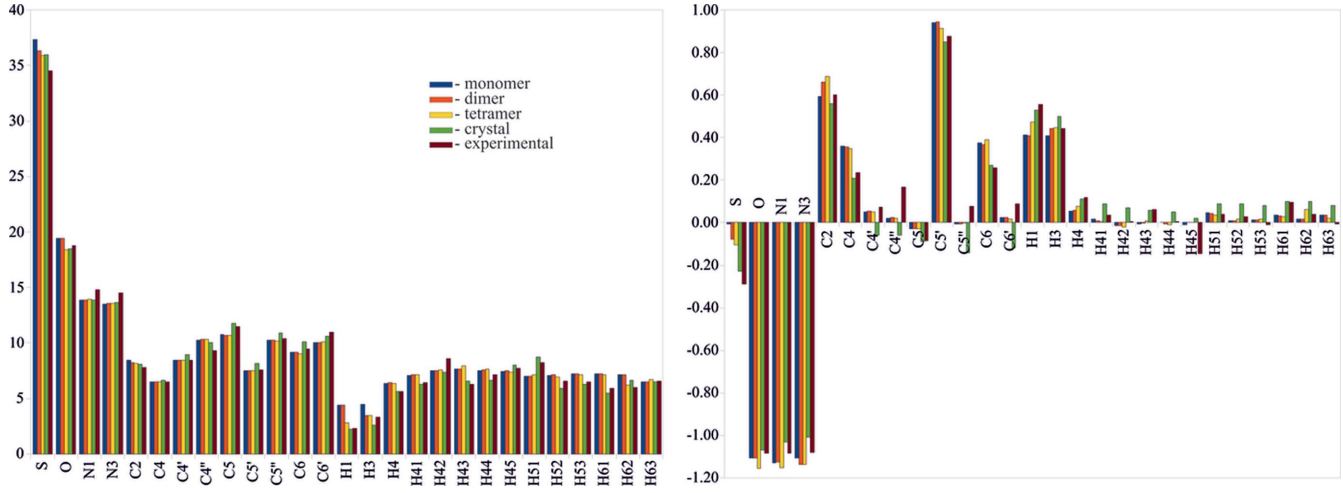

Figure 9
Atomic volumes (Å^3, left) and charges (e, right) for (1).

experimental one by not more than 0.008 a.u, and the Laplacian disagreement does not exceed 0.04 a.u.

The third type of non-covalent interactions occurs only in tetramers and crystals. It involves the O atom of the substituent in position 5 of the heterocyclic ring and the H atom of the second N—H residue. The theoretical and experimental parameters of the corresponding BCPs are again in very good agreement.

The deviations between theoretical and experimental QTAIMC bond descriptors for 'weak' non-covalent interactions are smaller than the corresponding values for the covalent bonds reported elsewhere (Rykounov & Tsirelson, 2009). Therefore, the results of quantum-chemical calculations or X-ray diffraction experiments for non-covalent interactions can be used without any additional correction for the prediction of chemical properties of the corresponding moieties.

3.3. Transferability of the atomic properties

The atomic volumes and integrated charges are given in Figs. 9–11 and Tables S8–S10. The absolute values of the integral $\int_{\Omega}\nabla^2\rho(\mathbf{r})\mathrm{d}V$ were less than 5×10^{-4} a.u. for each atom, which confirms the accuracy of the zero-flux surface determinations. As the integrated atomic characteristics derived from the ED are much less affected by the deficiencies of the multipole model (Rykounov & Tsirelson, 2009), these characteristics obtained from experiment and quantum-chemical calculations are in better agreement than the BCP properties. To examine how the intermolecular interactions influence the selected atomic properties, we compared these characteristics for the monomer, dimer, tetramer and crystal theoretical calculations with the corresponding experimental values.

For (1) the average deviation of theoretical atomic volumes from experiment is 0.81 Å^3 for the monomer, 0.74 Å^3 for the dimer, 0.62 Å^3 for the tetramer and 0.50 Å^3 for the crystal. The corresponding standard deviations (SD) are 0.62, 0.55, 0.44 and 0.34 Å^3. The mean atomic charge difference is 0.06 e in the first three cases and 0.07 e in the fourth and SDs are 0.06, 0.05, 0.05 and 0.07 e. In (2) the averaged volume deviations are 0.72/0.58/0.50/0.33 Å^3 (SDs are 0.73, 0.59, 0.43 and 0.26 Å^3) and charge discrepancies are (SDs are 0.06 e everywhere) 0.07/0.07/0.06/0.06 e. For (3) they are 0.91/0.82/0.68/0.45 Å^3 (SDs are 0.76, 0.68, 0.50 and 0.54 Å^3) and 0.07/0.07/0.07/0.06 e (SDs are 0.05 e everywhere). Thus the agreement in atomic volumes gradually and noticeably improves for larger systems, while the average deviation of atomic charges remains practically unchanged. At the same time the quantitative estimations do not confirm with certainty that improvement of the results with cluster enlargement is statistically significant.

Let us now trace the changes in the atomic QTAIM descriptors due to the formation of a molecular cluster. The volumes of H atoms involved in intermolecular bonding are the most affected, for example H3 in (1) is 20% (1 Å^3) contracted in the dimer compared with a single molecule, but its charge is only 7% (0.03 e) different. For the S atom in the thioxocarbonyl group the opposite is true, the volumes being slightly different, but the charge difference is more substantial. It is known that the S atom frequently has different charges in *ab initio* calculations and the X-ray diffraction experimental electron-density analysis of the same compound (Allen *et al.*, 1997; Wood *et al.*, 2008). In single molecule quantum-chemical calculations (Platts *et al.*, 1996; Gonzalez *et al.*, 1997; Rykounov & Tsirelson, 2009), this atom has approximately zero charge, whereas it is commonly about −0.3 e in crystal calculations (Allen *et al.*, 1997; Wood *et al.*, 2008). One of the origins of this discrepancy is the use of different models to obtain the electron-density characteristics from experimental data than from theoretical calculations. Apparently, this is not the only reason. In our theoretical calculations for a single molecule of (1) the sulfur-integrated atomic charge is −0.01 e, while the experimental value is −0.29 e. For (3) the corresponding values are −0.01 and −0.23 e. The value of the S atom charge in dimers of (1) and (3) is −0.08 and −0.09 e.

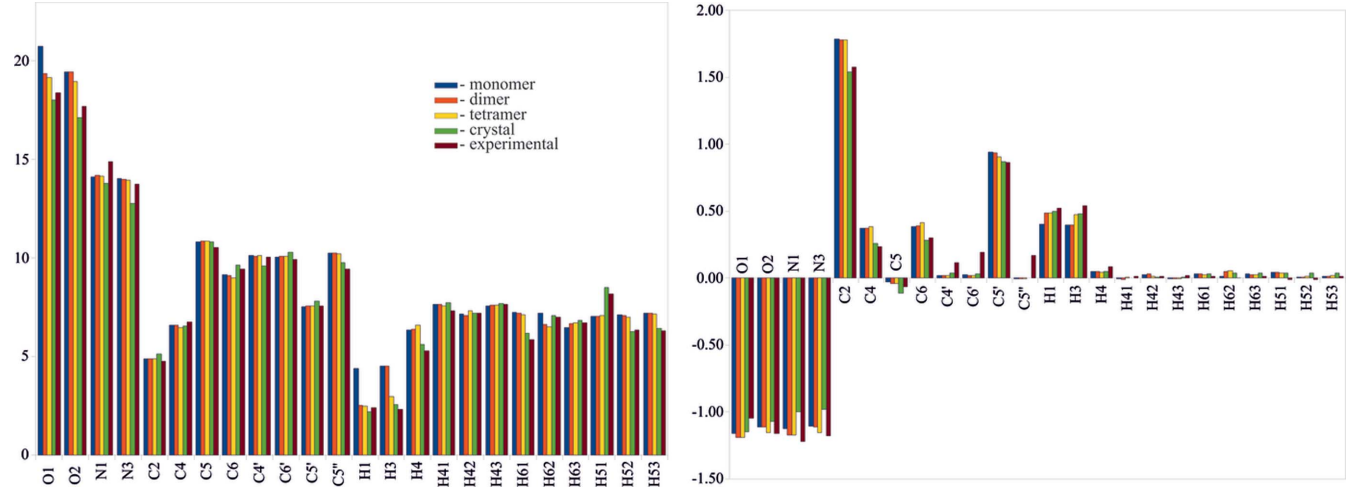

Figure 10
Atomic volumes (Å^3, left) and charges (e, right) for (2).

Corresponding values for the tetramers are −0.11 and −0.12 e. These results show that the difference in atomic charges between theoretical and experimental data is considerably less for molecular dimers than for a single molecule. Thus, for the evaluation of the atomic charge it is reasonable to construct molecular ensembles and consider the corresponding cluster instead of single molecules, at least for atoms directly involved in intermolecular interactions.

To verify the significance of the change in the atomic charge on sulfur in the transition from monomer to dimer, geometry optimization (DFT B3LYP/6-311++G**) followed by a QTAIMC analysis has been performed for thiourea – a compound which does not contain the heterocyclic ring and side-chain atoms. We note the closeness of the atomic charge and volume values for the S atom obtained from quantum-chemical calculations for the thiourea molecule and the hydropyrimidine derivatives examined in this work. The value of the S atom charge increases from −0.01 e for the monomer to −0.10 e in the thiourea dimer, which is in excellent agreement with the corresponding results for (1) and (3). Therefore, we can conclude that the negative charge of the S atom in a solid is partially determined by its environment.

The next observation is the distribution of electronic charge within the N—H···S═C fragment. While the total charge of this moiety remains practically the same, the value of the atomic charge for individual atoms is changed by up to 0.1 e on dimer formation. Together with the decrease in the S-atom charge, more positive charge values are observed not only for the H atom in the N—H fragment, but also for the C atom. That may be significant in the early stages of nucleophilic addition to the carbonyl group when compounds aggregated into molecular dimers would be more reactive than individual molecules. Thus, in the present study the more negative charge of the S atom obtained from the experiments most probably results from electron charge redistribution due to the formation of intermolecular hydrogen bonds. This redistribution involves not only the terminal atoms, but also atoms of the hydropyrimidine ring which can thus influence the chemical reactivity of these compounds.

4. Summary

The results of this study can be summarized as follows. The experimentally derived atomic and bond QTAIMC descriptors are generally transferable within chemically close structures such as the Biginelli compounds. Within the theoretical methods both bond and atomic QTAIMC characteristics are fully transferable between a single molecule, molecular dimer and tetramer. They are also transferable between the three-dimensional periodic electron-wavefunction calculations (with the single exception of the C—O bonds).

At the same time the experimental and theoretical QTAIMC descriptors for a crystal differ significantly for certain bond types. Primarily, this concerns the polar covalent bonds C═O and C—N, and also bonds of the *X*–H type (*X* = C, N). This results mainly from insufficient flexibility in the current electron density atom-centered multipole models leading to a bias in the bond-path longitudinal ED curvature, λ_3. The lack of multiple intermolecular interactions in the restricted-size model systems used in theoretical calculation may also influence the results.

We think that the analysis of theoretical electron density currently provides a reliable basis for the determination of the transferable QTAIMC descriptors for molecular structures. An empirical correction of the multipole-model experimental results for certain covalent bonds can be used to provide better transferability of the Laplacian-dependent QTAIMC descriptors.

This work was supported by the Russian Foundation for Basic Research, grant 10-03-00611a. We thank Professor A. D. Shutalev who has synthesized the compounds studied in this work, and Professor O. V. Shishkin for an opportunity to use

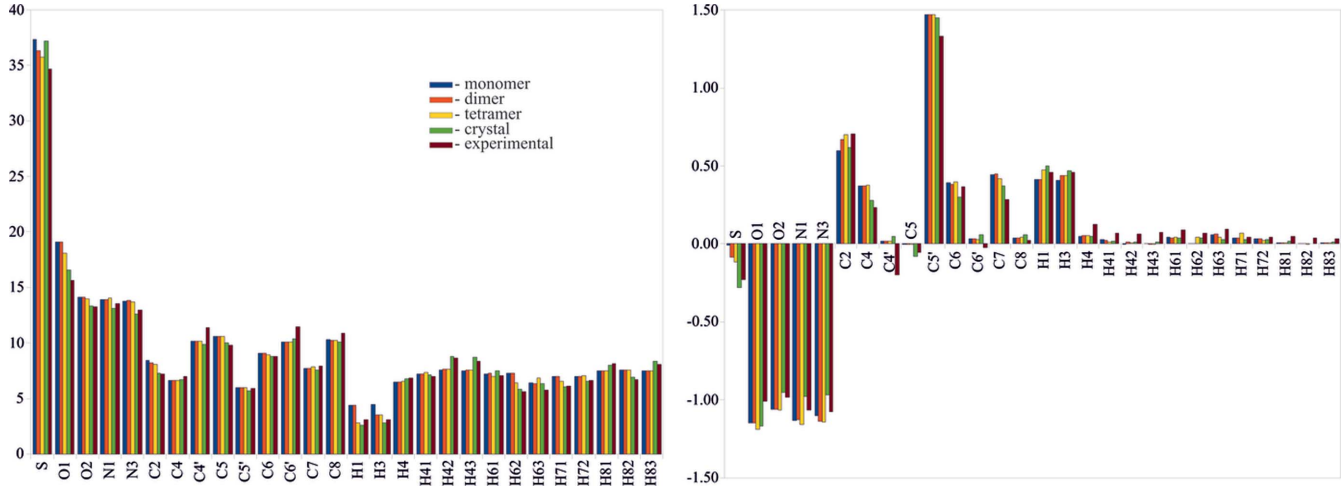

Figure 11
Atomic volumes (Å^3, left) and charges (e, right) for (3).

the computing facilities of the Ukrainian–American Laboratory of Computational Chemistry.

References

Abramov, Y. A., Volkov, A. V. & Coppens, P. (1999). *Chem. Phys. Lett.* **311**, 81–86.

Allen, F. H., Bird, C. M., Rowland, R. S. & Raithby, P. R. (1997). *Acta Cryst.* B**53**, 680–695.

Atwal, K. S., Swanson, B. N., Unger, S. E., Floyd, D. M., Moreland, S., Hedberg, A. & O'Reilly, B. C. (1991). *J. Med. Chem.* **34**, 806–811.

Bader, R. F. W. (1990). *Atoms in Molecules: A Quantum Theory. The International Series of Monographs of Chemistry*, edited by J. Halpen & M. L. H. Green. Oxford: Clarendon Press.

Bader, R. F. W. (2005). *Monatsh. Chem.* **136**, 819–854.

Barrow, J. C. *et al.* (2000). *J. Med. Chem.* **43**, 2703–2718.

Biginelli, P. (1893). *Gazz. Chim. Ital.* **23**, 360–413.

Blessing, R. H. (1987). *Cryst. Rev.* **1**, 3–58.

Blessing, R. H. (1989). *J. Appl. Cryst.* **22**, 396–397.

Blessing, R. H. (1995). *Acta Cryst.* A**51**, 33–38.

Breneman, C. M. & Rhem, M. (1997). *J. Comput. Chem.* **18**, 182–197.

Breneman, C. M. & Wiberg, K. B. (1990). *J. Comput. Chem.* **11**, 361–373.

Bürgi, H.-B., Capelli, S., Goeta, A. E., Howard, J. A. K., Spackman, M. A. & Yufit, D. S. (2002). *Chem. Eur. J.* **8**, 3512–3521.

Burnett, M. N. & Johnson, C. K. (1996). *ORTEP*III, Report ORNL-6895. Oak Ridge National Laboratory, Tennessee, USA.

Bytheway, I., Chandler, G. S. & Figgis, B. N. (2002). *Acta Cryst.* A**58**, 451–459.

Carvalho, M. F. de, Mosquera, R. A. & Rivelino, R. (2007). *Chem. Phys. Lett.* **445**, 117–124.

Castillo, N., Matta, C. F. & Boyd, R. J. (2005). *Chem. Phys. Lett.* **409**, 265–269.

Chandler, G. S. & Spackman, M. A. (1982). *Acta Cryst.* A**38**, 225–239.

Chang, C. & Bader, R. F. W. (1992). *J. Phys. Chem.* **96**, 1654–1662.

Coppens, P. & Volkov, A. (2004). *Acta Cryst.* A**60**, 357–364.

Destro, R., Soave, R. & Barzaghi, M. (2008). *J. Phys. Chem. B*, **112**, 5163–5174.

Dittrich, B., Koritsanszky, T. & Luger, P. (2004). *Angew. Chem. Int. Ed.* **43**, 2718–2721.

Dittrich, B., Koritsanszky, T., Volkov, A., Mebs, S. & Luger, P. (2007). *Angew. Chem. Int. Ed.* **46**, 2935–2938.

Dittrich, B., Scheins, S., Paulmann, C. & Luger, P. (2003). *J. Phys. Chem. A*, **107**, 7471–7474.

Dominiak, P. M., Volkov, A., Li, X., Messerschmidt, M. & Coppens, P. (2007). *J. Chem. Theory Comput.* **3**, 232–247.

Fabian, W. M. F., Semones, M. A. & Kappe, C. O. (1998). *J. Mol. Struct. THEOCHEM*, **432**, 219–228.

Flaig, R., Koritsanszky, T., Dittrich, B., Wagner, A. & Luger, P. (2002). *J. Am. Chem. Soc.* **124**, 3407–3417.

Fournier, B., Bendeif, E.-E., Guillot, B., Podjarny, A., Lecomte, C. & Jelsch, C. (2009). *J. Am. Chem. Soc.* **131**, 10929–10941.

Frisch, M. J. *et al.* (2003). *GAUSSIAN*03, Revision A.1. Gaussian Inc., Pittsburgh, PA.

Gatti, C. (1999). *TOPOND*98. CNR-ISTM, Milano, Italy.

Gonzalez, L., Mo, O. & Yanez, M. (1997). *J. Phys. Chem. A*, **101**, 9710–9719.

Gonzalez Moa, M. J., Mandado, M. & Mosquera, R. A. (2008). *Chem. Phys. Lett.* **428**, 255–261.

Grover, G. J., Dzwonczyk, S., McMullen, D. M., Normandin, D. E., Parham, C. S., Sleph, P. G. & Moreland, S. (1995). *J. Cardiovasc. Pharmacol.* **26**, 289–294.

Guillot, B., Muzet, N., Artacho, E., Lecomte, C. & Jelsch, C. (2003). *J. Phys. Chem. B*, **107**, 9109–9121.

Gurskaya, G. V., Zavodnik, V. E. & Shutalev, A. D. (2003*a*). *Crystallogr. Rep.* **48**, 92–97.

Gurskaya, G. V., Zavodnik, V. E. & Shutalev, A. D. (2003*b*). *Crystallogr. Rep.* **48**, 416–421.

Haggarty, S. J., Mayer, T. U., Miyamoto, D. T., Fathi, R., King, R. W., Mitchison, T. J. & Schreiber, S. L. (2000). *Chem. Biol.* **7**, 275–286.

Hansen, N. K. & Coppens, P. (1978). *Acta Cryst.* A**34**, 909–921.

Hibbs, D. E., Austin-Woods, C. J., Platts, J. A., Overgaard, J. & Turner, P. (2003). *Chem. Eur. J.* **9**, 1075–1084.

Hibbs, D. E., Hanrahan, J. R., Hursthouse, M. B., Knight, D. W., Overgaard, J., Turner, P., Piltz, R. O. & Waller, M. P. (2003). *Org. Biomol. Chem.* **1**, 1034–1040.

Hirshfeld, F. L. (1976). *Acta Cryst.* A**32**, 239–244.

Housset, D., Benabicha, F., Pichon-Pesme, V., Jelsch, C., Maierhofer, A., David, S., Fontecilla-Camps, J. C. & Lecomte, C. (2000). *Acta Cryst.* D**56**, 151–160.

Hübschle, C. B., Dittrich, B., Grabowsky, S., Messerschmidt, M. & Luger, P. (2008). *Acta Cryst.* B**64**, 363–374.

Hübschle, C. B., Luger, P. & Dittrich, B. (2007). *J. Appl. Cryst.* **40**, 623–627.

Iversen, B. B., Larsen, F. K., Figgis, B. N. & Reynolds, P. A. (1997). *J. Chem. Soc. Dalton Trans.* pp. 2227–2240.

Jelsch, C., Pichon-Pesme, V., Lecomte, C. & Aubry, A. (1998). *Acta Cryst.* D**54**, 1306–1318.

Kalinowski, R., Dittrich, B., Hübschle, C. B., Paulmann, C. & Luger, P. (2007). *Acta Cryst.* B**63**, 753–767.

Kappe, C. O., Fabian, W. M. F. & Semones, M. A. (1997). *Tetrahedron*, **53**, 2803–2816.

Kappe, C. O., Shishkin, O. V., Uray, G. & Verdino, P. (2000). *Tetrahedron*, **56**, 1859–1862.

Keith, T. A. (2009). *AIMAll*, Version 09.02.01, http://aim.tkgristmill.com.

Koritsanszky, T., Volkov, A. & Coppens, P. (2002). *Acta Cryst.* A**58**, 464–472.

Lecomte, C., Guillot, B., Jelsch, C. & Podjarny, A. (2005). *Int. J. Quantum Chem.* **101**, 624–634.

Lorenzo, L., Gonzalez Moa, M. J., Mandado, M. & Mosquera, R. A. (2006). *J. Chem. Inf. Model.* **46**, 2056–2065.

Macchi, P. & Coppens, P. (2001). *Acta Cryst.* A**57**, 656–662.

Matta, C. F. (2010). *J. Comput. Chem.* **31**, 1297–1311.

Matta, C. F. & Arabi, A. A. (2011). *Future Med. Chem.* **3**, 969–994.

Matta, C. F. & Bader, R. F. (2000). *Proteins*, **40**, 310–329.

Matta, C. F. & Bader, R. F. (2002). *Proteins*, **48**, 519–538.

Matta, C. F. & Bader, R. F. (2003). *Proteins*, **52**, 360–399.

Matta, C. F., Castillo, N. & Boyd, R. J. (2006). *J. Phys. Chem. B*, **110**, 563–578.

Milanesio, M., Bianchi, R., Ugliengo, P., Roetti, C. & Viterbo, D. (1997). *J. Mol. Struct. THEOCHEM*, **419**, 139–154.

Nagarathnam, D. *et al.* (1999). *J. Med. Chem.* **42**, 4764–4777.

O'Brien, S. E. & Popelier, P. L. A. (1999). *Can. J. Chem.* **77**, 28–36.

O'Brien, S. E. & Popelier, P. L. (2001). *J. Chem. Inf. Comput. Sci.* **41**, 764–775.

Pakiari, A. H., Farrokhnia, M. & Azami, S. M. (2008). *Chem. Phys. Lett.* **457**, 211–215.

Parini, E. V., Tsirelson, V. G. & Ozerov, R. P. (1985). *Sov. Phys. Crystallogr.* **30**, 497–502.

Pichon-Pesme, V., Lecomte, C. & Lachekar, H. (1995). *J. Phys. Chem.* **99**, 6242–6250.

Platts, J. A., Howard, S. T. & Bracke, B. R. F. (1996). *J. Am. Chem. Soc.* **118**, 2726–2733.

Ponec, R. & Gatti, C. (2009). *Inorg. Chem.* **48**, 11024–11031.

Popelier, P. L. A. (1999). *J. Phys. Chem. A*, **103**, 2883–2890.

Potemkin, V. A., Grishina, M. A. & Bartashevich, E. V. (2008). *J. Struct. Chem.* **48**, 153–158.

Protas, J. (1997). *MOLDOS*97/*MOLLY*, MS DOS Updated Version. Personal communication.

Rincon, D. A., Cordeiro, M. N. D. S., Mosquera, R. A. & Borges, F. (2009). *Chem. Phys. Lett.* **467**, 249–254.

Rovnyak, G. C., Kimball, S. D., Beyer, B., Cucinotta, G., DiMarco, J. D., Gougoutas, J., Hedberg, A., Malley, M., McCarthy, J. P., Zhang, R. & Moreland, S. (1995). *J. Med. Chem.* **38**, 119–129.

Rykounov, A. A. & Tsirelson, V. G. (2009). *J. Mol. Struct. THEOCHEM*, **906**, 11–24.
Saunders, V. R., Dovesi, R., Roetti, C., Causà, M., Harrison, N. M., Orlando, R. & Zicovich-Wilson, C. M. (1998). *CRYSTAL* User's Manual, p. 98. University of Torino, Italy.
Scheins, S., Messerschmidt, M. & Luger, P. (2005). *Acta Cryst.* B**61**, 443–448.
Sheldrick, G. M. (2008). *Acta Cryst.* A**64**, 112–122.
Shishkin, O. V., Solomovich, E. V., Vakula, V. M. & Yaremenko, F. G. (1997). *Russ. Chem. Bull.* **46**, 1838–1843.
Shutalev, A. D., Kishko, E. A., Sivova, N. V. & Kuznetsov, A. Yu. (1998). *Molecules*, **3**, 100–106.
Shutalev, A. D. & Kuksa, V. A. (1997). *Khim. Geterot. Soedin.* pp. 105–109 (in Russian).
Siemens (1996). *SMART* and *SAINT*. Siemens Analytical X-ray Instruments Inc., Madison, Wisconsin, USA.
Stash, A. I. (2003). *Proceedings of the 28th ISTC Japan Workshop on Frontiers of X-ray Diffraction Technologies in Russia/CIS*, pp. 147–153. Nagoya.
Stash, A. & Tsirelson, V. (2002). *J. Appl. Cryst.* **35**, 371–373.
Stash, A. I. & Tsirelson, V. G. (2005). *Cryst. Rep.* **50**, 177–184.
Tsirelson, V. G. (2002). *Acta Cryst.* B**58**, 632–639.
Tsirelson, V. G. & Ozerov, R. P. (1996). *Electron Density and Bonding in Crystals.* Bristol, Philadelphia: Institute of Physics.
Tsirelson, V. G., Stash, A. I., Potemkin, V. A., Rykounov, A. A., Shutalev, A. D., Zhurova, E. A., Zhurov, V. V., Pinkerton, A. A., Gurskaya, G. V. & Zavodnik, V. E. (2006). *Acta Cryst.* B**62**, 676–688.
Uray, G., Verdino, P., Belaj, F., Kappe, C. O. & Fabian, W. M. (2001). *J. Org. Chem.* **66**, 6685–6694.
Vener, M. V., Egorova, A. N., Fomin, D. P. & Tsirelson, V. G. (2007). *Chem. Phys. Lett.* **440**, 279–285.
Volkov, A., Abramov, Y., Coppens, P. & Gatti, C. (2000). *Acta Cryst.* A**56**, 332–339.
Volkov, A. & Coppens, P. (2001). *Acta Cryst.* A**57**, 395–405.
Volkov, A., Koritsanszky, T., Li, X. & Coppens, P. (2004). *Acta Cryst.* A**60**, 638–639.
Volkov, A., Messerschmidt, M. & Coppens, P. (2007). *Acta Cryst.* D**63**, 160–170.
Vries, R. Y. de, Feil, D. & Tsirelson, V. G. (2000). *Acta Cryst.* B**56**, 118–123.
Walker, P. D., Arteca, G. A. & Mezey, P. G. (1991). *J. Comput. Chem.* **12**, 220–230.
Walker, P. D. & Mezey, P. G. (1994). *J. Am. Chem. Soc.* **116**, 12022–12032.
Whitehead, C. E., Breneman, C. M., Sukumar, N. & Ryan, M. D. (2003). *J. Comput. Chem.* **24**, 512–529.
Wiberg, K. B., Bader, R. F. W. & Lau, C. D. H. (1987). *J. Am. Chem. Soc.* **109**, 1001–1012.
Wood, P. A., Pidcock, E. & Allen, F. H. (2008). *Acta Cryst.* B**64**, 491–496.
Zarychta, B., Pichon-Pesme, V., Guillot, B., Lecomte, C. & Jelsch, C. (2007). *Acta Cryst.* A**63**, 108–125.
Zavodnik, V. E., Shutalev, A. D., Gurskaya, G. V., Stash, A. I. & Tsirelson, V. G. (2005*a*). *Acta Cryst.* E**61**, o468–o470.
Zavodnik, V. E., Shutalev, A. D., Gurskaya, G. V., Stash, A. I. & Tsirelson, V. G. (2005*b*). *Acta Cryst.* E**61**, o365–o367.
Zefirov, N. S. & Palyulin, V. A. (2002). *J. Chem. Inf. Comput. Sci.* **42**, 1112–1122.
Zhurova, E. A., Matta, C. F., Wu, N., Zhurov, V. V. & Pinkerton, A. A. (2006). *J. Am. Chem. Soc.* **128**, 8849–8861.
Zhurova, E. A., Stash, A. I., Tsirelson, V. G., Zhurov, V. V., Bartashevich, E. V., Potemkin, V. A. & Pinkerton, A. A. (2006). *J. Am. Chem. Soc.* **128**, 14728–14734.